Analyzing the Diversity of Constrained Multiobjective Optimization Test Suites

Aljoša Vodopija
aljosa.vodopija@ijs.si
Jožef Stefan Institute and
Jožef Stefan International
Postgraduate School
Jamova cesta 39
Ljubljana, Slovenia

Tea Tušar
tea.tusar@ijs.si
Jožef Stefan Institute and
Jožef Stefan International
Postgraduate School
Jamova cesta 39
Ljubljana, Slovenia

Bogdan Filipič
bogdan.filipic@ijs.si
Jožef Stefan Institute and
Jožef Stefan International
Postgraduate School
Jamova cesta 39
Ljubljana, Slovenia

ABSTRACT

A well-designed test suite for benchmarking novel optimizers for constrained multiobjective optimization problems (CMOPs) should be diverse enough to detect both the optimizers' strengths and shortcomings. However, until recently there was a lack of methods for characterizing CMOPs, and measuring the diversity of a suite of problems was virtually impossible. This study utilizes the landscape features proposed in our previous work to characterize frequently used test suites for benchmarking optimizers in solving CMOPs. In addition, we apply the t-distributed Stochastic Neighbor Embedding (t-SNE) dimensionality reduction approach to reveal the diversity of these test suites. The experimental results indicate which ones express sufficient diversity.

KEYWORDS

constrained multiobjective optimization, benchmarking, landscape feature, t-SNE

1 INTRODUCTION

Real-world optimization problems frequently involve multiple objectives and constraints. These problems are called *constrained multiobjective optimization problems* (CMOPs) and have been gaining a lot of attention in the last years [13]. As with other theoretically-oriented optimization studies, a crucial step in testing novel algorithms in constrained multiobjective optimization is the preparation of a benchmark test.

One of the key elements of a benchmark test is the selection of suitable test CMOPs [1]. A well-designed benchmark suite should include "a wide variety of problems with different characteristics" [1]. This way the benchmark problems are *diverse* enough to "highlight the strengths as well as weaknesses of different algorithms" [1]. However, until recently there existed only few and limited techniques proposed to explore CMOPs [13]. For this reason, the test suites of CMOPs were insufficiently understood and measuring their diversity was virtually impossible.

To overcome this situation, in our previous work [13], we experimented with various exploratory landscape analysis (ELA) techniques and proposed 29 landscape features to characterize CMOPs, including their *violation landscapes*—a similar concept as the fitness landscape where fitness is replaced by the *overall constraint violation*.

In this study, we employ the landscape features proposed in [13] to express and discuss the diversity of frequently used test suites of CMOPs. This is achieved by firstly computing the landscape features and then employing the t-distributed Stochastic Neighbor Embedding (t-SNE), a dimensionality reduction technique, to embed the 29-D CMOP feature space into the 2-D space. Note that due to space limitations, only selected results are shown in this paper. The complete results can be found online[1].

The rest of this paper is organized as follows. Section 2 provides the theoretical background. In Section 3, we present the landscape features and the t-SNE algorithm. Section 4 is dedicated to the experimental setup, while the results are discussed in Section 5. Finally, Section 6 summarizes the study and provides an idea for future work.

2 THEORETICAL BACKGROUND

A CMOP can be formulated as:

$$\begin{aligned} \text{minimize} \quad & f_m(x), \quad m = 1, \ldots, M \\ \text{subject to} \quad & g_i(x) \leq 0, \quad i = 1, \ldots, I \end{aligned} \tag{1}$$

where $x = (x_1, \ldots, x_D)$ is a *search vector*, $f_m : S \to \mathbb{R}$ are *objective functions*, $g_i : S \to \mathbb{R}$ *constraint functions*, $S \subseteq \mathbb{R}^D$ is a *search space* of dimension D, and M and I are the numbers of objectives and constraints, respectively.

If a solution x satisfies all the constraints, $g_i(x) \leq 0$ for $i = 1, \ldots, I$, then it is a *feasible* solution. For each of the constraints g_i we can define the *constraint violation* as $v_i(x) = \max(0, g_i(x))$. In addition, an *overall constraint violation* is defined as

$$v(x) = \sum_i^I v_i(x). \tag{2}$$

A solution x is feasible iff $v(x) = 0$.

A feasible solution $x \in S$ is said to *dominate* a solution $y \in S$ if $f_m(x) \leq f_m(y)$ for all $1 \leq m \leq M$, and $f_m(x) < f_m(y)$ for at least one $1 \leq m \leq M$. In addition, $x^* \in S$ is a *Pareto-optimal solution* if there exists no $x \in S$ that dominates x^*. All feasible solutions represent a *feasible region*, $F = \{x \in S \mid v(x) = 0\}$. Besides, all nondominated feasible solutions form a *Pareto-optimal set*, S_o. The image of the Pareto-optimal set is the *Pareto front*, $P_o = \{f(x) \mid x \in S_o\}$. A connected component (a maximal connected subset with respect to the inclusion order) of the feasible region is called a *feasible component*, $\mathcal{F} \subseteq F$.

In [13], we introduced analogous terms from the perspective of the overall constraint violation. A *local minimum-violation solution* is thus a solution x^* for which exists a $\delta > 0$ such that $v(x^*) \leq v(x)$ for all $x \in \{x \mid d(x^*, x) \leq \delta\}$. If there is no other solution $x \in S$ for which $v(x^*) > v(x)$, then x^* is a

---

[1]https://vodopijaaljosa.github.io/cmop-web/

(global) minimum-violation solution. We denoted the set of all local minimum-violation solutions by F_l and called a connected component $\mathcal{M} \subseteq F_l$ a *local minimum-violation component*.

In order to express the modality of a violation landscape, we defined a local search procedure to be a mapping from the search space to the set of local minimum-violation solutions, $\mu : S \rightarrow F_l$, such that $\mu(x) = x$ for all $x \in F_l$. A *basin of attraction* of a local minimum-violation component $\mathcal{M}$ and local search μ is then a subset of S in which μ converges towards a solution from $\mathcal{M}$, i.e., $\mathcal{B}(\mathcal{M}) = \{x \in S \mid \mu(x) \in \mathcal{M}\}$. The violation landscape is *unimodal* if there is only one basin in S and *multimodal* otherwise.

3 METHODOLOGY

3.1 ELA Features

The landscape features used in this study were introduced in our previous work [13] and can be categorized into four groups: space-filling design, information content, random walk and adaptive walk features. They are summarized in Table 1.

The space-filling design features are used to quantify the feasible components, the relationship between the objectives and constraints, and measure the feasibility ratio and proportion of boundary Pareto-optimal solutions. Next, the information content features are mainly used to express the smoothness and ruggedness of violation landscapes. They are derived by analyzing the entropy of sequences of overall violation values as obtained from a random sampling of the search space. Then, the random walk features considered in this study are used to quantify the number of boundary crossings from feasible to infeasible regions. They are used to categorize the degree of segmentation of the feasible region. Finally, features from the last group are derived from adaptive walks through the search space. They are used to describe various aspects of basins of attraction in the violation landscapes.

3.2 Dimensionality Reduction with t-SNE

The t-SNE algorithm is a popular nonlinear dimensionality reduction technique designed to represent high-dimensional data in a low-dimensional space, typically the 2-D plane [12]. First, it converts similarities between data points to distributions. Then, it tries to find a low-dimensional embedding of the points that minimizes the divergence between the two distributions that measure neighbor similarity—one in the original space and the other in the projected space. This means that t-SNE tries to preserve the local relationships between neighboring points, while the global structure is generally lost.

Finding the best embedding is an optimization problem with a non-convex fitness function. To solve it, t-SNE uses a gradient descent method with a random starting point, which means that different runs can yield different results. The output of t-SNE depends also on other parameters, such as the *perplexity* (similar to the number of nearest neighbors in other graph-based dimensionality reduction techniques), *early exaggeration* (separation of clusters in the embedded space) and *learning rate* (also called ε). The gradients can be computed exactly or estimated using the Barnes-Hut approximation, which substantially accelerates the method without degrading its performance [11].

4 EXPERIMENTAL SETUP

We studied eight suites of CMOPs which are most frequently used in the literature. These are CTP [2], CF [14], C-DTLZ [5], NCTP [7], DC-DTLZ [8], LIR-CMOP [3], DAS-CMOP [4], and

Table 1: The ELA features used to characterize CMOPs categorized into four groups: space-filling design, information content, random walk, and adaptive walk [13].

Space-filling design features	
$N_{\mathcal{F}}$	Number of feasible components
$\mathcal{F}_{\min}$	Smallest feasible component
$\mathcal{F}_{\mathrm{med}}$	Median feasible component
$\mathcal{F}_{\max}$	Largest feasible component
$O(\mathcal{F}_{\max})$	Proportion of Pareto-optimal solutions in $\mathcal{F}_{\max}$
$\mathcal{F}_{\mathrm{opt}}$	Size of the "optimal" feasible component
ρ_{F}	Feasibility ratio
$\rho_{\min}$	Minimum correlation
$\rho_{\max}$	Maximum correlation
$\rho_{\partial S_o}$	Proportion of boundary Pareto-optimal solutions
Information content features	
$H_{\max}$	Maximum information content
ε_s	Settling sensitivity
M_0	Initial partial information
Random walk features	
$(\rho_{\partial F})_{\min}$	Minimal ratio of feasible boundary crossings
$(\rho_{\partial F})_{\mathrm{med}}$	Median ratio of feasible boundary crossings
$(\rho_{\partial F})_{\max}$	Maximal ratio of feasible boundary crossings
Adaptive walk features	
$N_{\mathcal{B}}$	Number of basins
$\mathcal{B}_{\min}$	Smallest basin
$\mathcal{B}_{\mathrm{med}}$	Median basin
$\mathcal{B}_{\max}$	Largest basin
$(\mathcal{B}_{\mathrm{F}})_{\min}$	Smallest feasible basin
$(\mathcal{B}_{\mathrm{F}})_{\mathrm{med}}$	Median feasible basin
$(\mathcal{B}_{\mathrm{F}})_{\max}$	Largest feasible basin
$\cup \mathcal{B}_{\mathrm{F}}$	Proportion of feasible basins
$v(\mathcal{B})_{\mathrm{med}}$	Median constraint violation over all basins
$v(\mathcal{B})_{\max}$	Maximum constraint violation of all basins
$v(\mathcal{B}_{\max})$	Constraint violation of $\mathcal{B}_{\max}$
$O(\mathcal{B}_{\max})$	Proportion of Pareto-optimal solutions in $\mathcal{B}_{\max}$
$\mathcal{B}_{\mathrm{opt}}$	Size of the "optimal" basin

MW [9]. In addition, we included also a novel suite named RCM [6]. In contrast to other suites which consist of artificial test problems, RCM contains 50 instances of real-world CMOPs based on physical models. Note that we actually used only 11 RCM problems, since only continuous and low-dimensional problems were suitable for our analysis. We considered three dimensions of the search space: 2, 3, 5. It is to be noted that large-scale CMOPs were not taken into account since the methodology described in Section 3 is not sufficiently scalable. This limits our results to low-dimensional CMOPs. Table 2 shows the basic characteristics of the studied test suites.

For dimensionality reduction, we used the t-SNE implementation from the *scikit-learn* Python package [10] with default parameter values. That is, we used the Euclidean distance metric, random initialization of the embedding, perplexity of 30, early exaggeration of 12, learning rate of 200, the maximum number of iterations of 1000, and the maximum number of iterations without progress before aborting of 300. The gradient was computed by the Barnes-Hut approximation with the angular size of 0.5.

5 RESULTS AND DISCUSSION

The results obtained by t-SNE are shown in Figures 1 and 2. Specifically, the figures show the 2-D embedding of the 29-D

Table 2: Characteristics of test suites: number of problems, dimension of the search space D, number of objectives M, and number of constraints I. The characteristics of selected RCM problems are shown in parentheses.

Test suite	#problems	D	M	I
CTP [2]	8	*	2	2, 3
CF [14]	10	*	2, 3	1, 2
C-DTLZ [5]	6	*	*	1, *
NCTP [7]	18	*	2	1, 2
DC-DTLZ [8]	6	*	*	1, *
DAS-CMOP [4]	9	*	2, 3	7, 11
LIR-CMOP [3]	14	*	2, 3	2, 3
MW [9]	14	*	2, *	1–4
RCM [6]	50 (11)	2–34 (2–5)	2–5	1–29 (1–8)

*Scalable parameter.
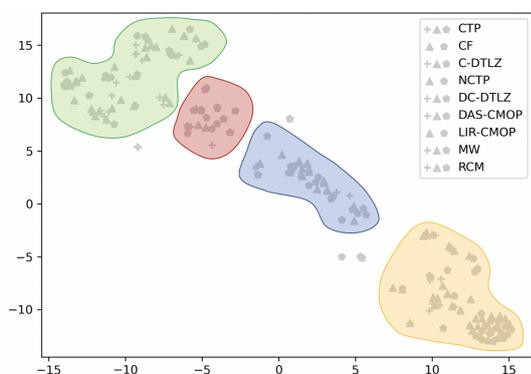
Figure 1: Embedding of the feature space as obtained by t-SNE. The four regions are depicted in green, red, blue, and orange. The points that are not contained in any region are considered to be outliers.

feature space consisting of the landscape features presented in Table 1. Each subfigure in Figure 2 corresponds to one of the test suites. For example, Figure 2a exposes the embedding of the CTP suite in blue, while the gray points correspond to the rest of the test suites. Points with a shape of a plus (+) correspond to CMOPs with two variables, points with a shape of a triangle (▲) to CMOPs with three variables, and points with a shape of a pentagon (⬠) to CMOPs with five variables.

An additional analysis shows that the embedding of the feature space can be, based on the corresponding characteristics, split into four regions: green, red, blue and yellow (Figure 1). The green region corresponds to CMOPs with severe violation multimodality, small basins of attraction, and rugged violation landscapes. The red region corresponds to CMOPs with moderate violation multimodality, rugged violation landscapes, and small feasibility ratios. The blue region corresponds to relatively low violation multimodality, rugged violation landscapes, small feasibility ratios, and positive correlations between objectives and constraints. Finally, the yellow region corresponds to unimodal CMOPs with large feasible components, smooth violation landscapes, and large feasible regions.

As we can see from Figure 2a, almost all CTP problems are located in the orange region. Therefore, many relevant characteristics are poorly represented by CTP, e.g., violation multimodality, small feasibility ratios, etc. Similarly, NCTP fails to sufficiently

represent severe multimodality since it contains no problems from the green region (Figure 2d). On the other hand, DC-DTLZ, LIR-CMOP, and MW are biased towards highly multimodal violation landscapes or those with small basins of attraction (Figure 2e, Figure 2g, and Figure 2h). Nevertheless, MW is one of the most diverse suites considering other characteristics (Figure 2h).

The C-DTLZ and DAS-CMOP suites are mainly located in the green and orange regions and fail to sufficiently represent the characteristics of the red and blue regions.

Finally, the results show that CF and RCM are well spread through the whole embedded feature space (Figure 2b and Figure 2i). As we can see, they have at least one representative CMOP instance in each region. Therefore, CF and RCM are the most diverse test suites according to the employed landscape features.

6 CONCLUSIONS

In this paper, we analyzed the diversity of the frequently used test suites for benchmarking optimizers in solving CMOPs. For this purpose, we considered 29 landscape features for CMOPs that were proposed in our previous work. In addition, the t-SNE algorithm was used to reduce the dimensionality of the feature space and reveal the diversity of the considered test suites.

The experimental results show that the most diverse test suites of CMOPs according to the applied landscape features are CF and RCM. Indeed, they include the widest variety of CMOPs with different characteristics. In addition, MW also proved to be a diverse suite except for unimodal CMOPs. Nevertheless, we suggest to consider CMOPs from various test suites for benchmarking optimizers in constrained multiobjective optimization.

One of the main limitations of our study is that only low-dimensional CMOPs were used in the analysis. Therefore, we were unable to adequately address the issue of scalability. For this reason, a crucial task that needs to be addressed in the feature is the extension of this work to large-scale CMOPs.

REFERENCES

[1] T. Bartz-Beielstein, C. Doerr, J. Bossek, S. Chandrasekaran, T. Eftimov, A. Fischbach, P. Kerschke, M. López-Ibáñez, K. M. Malan, J. H. Moore, B. Naujoks, P. Orzechowski, V. Volz, M. Wagner, and T. Weise. Benchmarking in optimization: Best practice and open issues. arXiv:2007.03488v2, (2020).

[2] K. Deb, A. Pratap, and T. Meyarivan. 2001. Constrained test problems for multi-objective evolutionary optimization. In *Evolutionary Multi-Criterion Optimization (EMO 2001)*, 284–298.

[3] Z. Fan, W. Li, X. Cai, H. Huang, Y. Fang, Y. You, J. Mo, C. Wei, and E. Goodman. 2019. An improved epsilon constraint-handling method in MOEA/D for CMOPs with large infeasible regions. *Soft Comput.*, 23, 23, 12491–12510. DOI: 10.1007/s00500-019-03794-x.

[4] Z. Fan, W. Li, X. Cai, H. Li, C. Wei, Q. Zhang, K. Deb, and E. Goodman. 2019. Difficulty adjustable and scalable constrained multiobjective test problem toolkit. *Evol. Comput.*, 28, 3, 339–378. DOI: 10.1162/evco-a-00259.
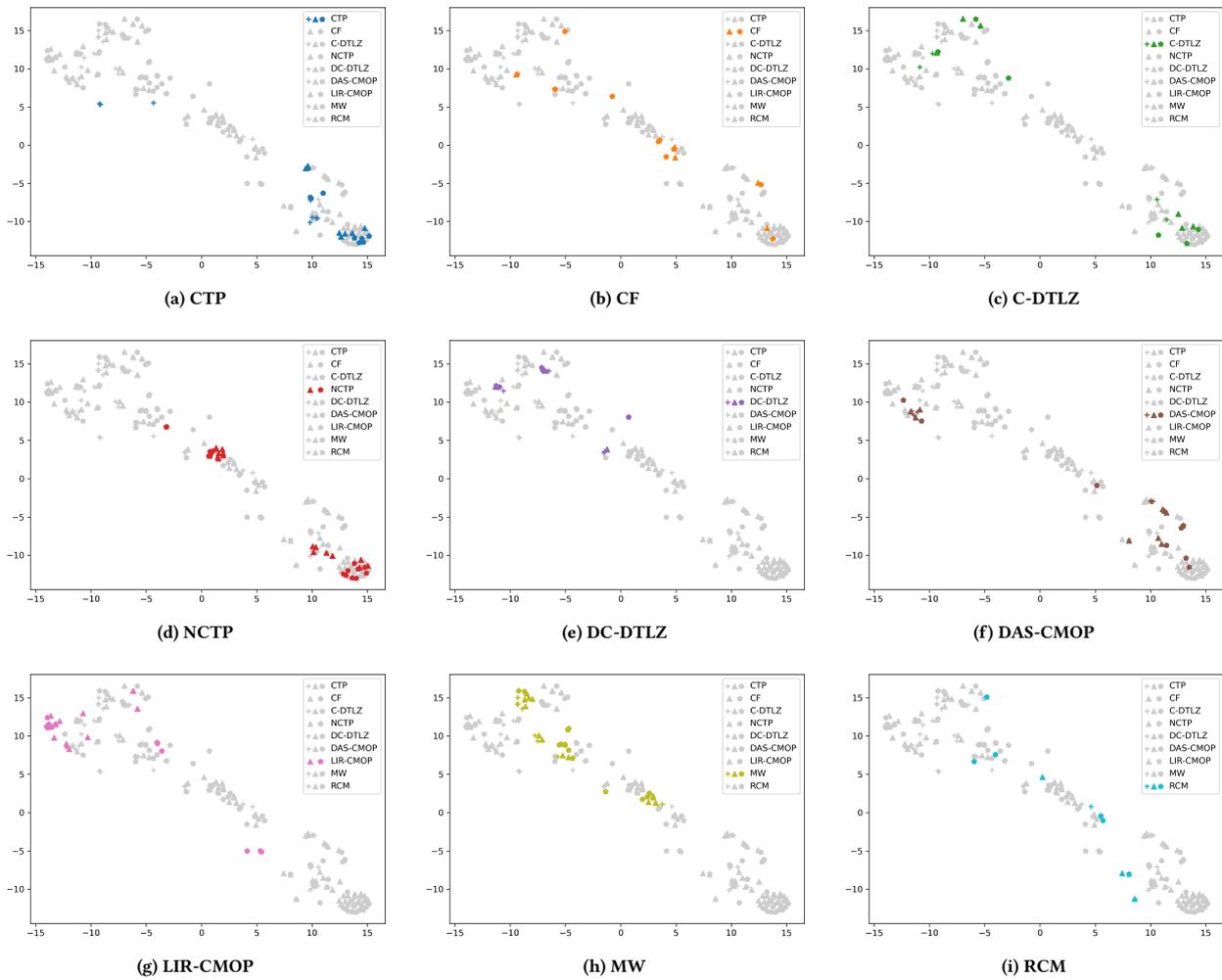
Figure 2: Embedding of the feature space as obtained by t-SNE. Each subfigure exposes the embedding of a selected suite.

[5] H. Jain and K. Deb. 2014. An evolutionary many-objective optimization algorithm using reference-point based non-dominated sorting approach, Part II: Handling constraints and extending to an adaptive approach. *IEEE Trans. Evol. Comput.*, 18, 4, 602−622. DOI: 10.1109/TEVC.2013.2281534.

[6] A. Kumar, G. Wu, M. Z. Ali, Q. Luo, R. Mallipeddi, P. N. Suganthan, and S. Das. 2020. A Benchmark-Suite of Real-World Constrained Multi-Objective Optimization Problems and some Baseline Results. Technical report. Indian Institute of Technology, Banaras Hindu University Campus, India.

[7] J. P. Li, Y. Wang, S. Yang, and Z. Cai. 2016. A comparative study of constraint-handling techniques in evolutionary constrained multiobjective optimization. In *IEEE Congress on Evolutionary Computation (CEC 2016)*, 4175−4182. DOI: 10.1109/CEC.2016.7744320.

[8] K. Li, R. Chen, G. Fu, and X. Yao. 2019. Two-archive evolutionary algorithm for constrained multiobjective optimization. *IEEE Trans. Evol. Comput.*, 23, 2, 303−315. DOI: 10.1109/TEVC.2018.2855411.

[9] Z. Ma and Y. Wang. 2019. Evolutionary constrained multiobjective optimization: Test suite construction and performance comparisons. *IEEE Trans. Evol. Comput.*, 23, 6, 972−986. DOI: 10.1109/TEVC.2019.2896967.

[10] F. Pedregosa, G. Varoquaux, A. Gramfort, V. Michel, B. Thirion, O. Grisel, M. Blondel, P. Prettenhofer, R. Weiss, V. Dubourg, J. Vanderplas, A. Passos, D. Cournapeau, M. Brucher, M. Perrot, and E. Duchesnay. 2011. Scikit-learn: machine learning in Python. *J. Mach. Learn. Res.*, 12, 2825−2830.

[11] L. van der Maaten. 2014. Accelerating t-SNE using tree-based algorithms. *J. Mach. Learn. Res.*, 15, 1, 3221−3245.

[12] L. van der Maaten and G. Hinton. 2008. Visualizing data using t-SNE. *J. Mach. Learn. Res.*, 9, 2579−2605.

[13] A. Vodopija, T. Tušar, and B. Filipič. Characterization of constrained continuous multiobjective optimization problems: A feature space perspective. arXiv:2109.04564, (2021).

[14] Q. Zhang, A. Zhou, S. Zhao, P. N. Suganthan, W. Liu, and S. Tiwari. 2008. Multiobjective optimization test instances for the CEC 2009 special session and competition. Technical report CES-487. The School of Computer Science and Electronic Engieering, University of Essex, UK.